

Scientifique.

<sup>1</sup>J. P. Hansen, G. M. Torrie, and P. Vieillefosse, to be published.<sup>2</sup>P. Vieillefosse and J. P. Hansen, *Phys. Rev. A* **12**, 1106 (1975).<sup>3</sup>P. Vieillefosse, *J. Phys. (Paris)* **38**, L43 (1977).<sup>4</sup>P. V. Giaquinta, M. Parrinello, and M. P. Tosi, *Phys. Chem. Liq.* **5**, 305 (1976).<sup>5</sup>J. P. Hansen, I. R. McDonald, and E. L. Pollock, *Phys. Rev. A* **11**, 1025 (1975).<sup>6</sup>This point is discussed by M. Baus, *Physica (Utrecht)* **79A**, 377 (1975).

## Fast-Ion Generation by Ion-Acoustic Turbulence in Spherical Laser Plasmas

P. M. Campbell, R. R. Johnson, F. J. Mayer, L. V. Powers, and D. C. Slater

*KMS Fusion, Inc., Ann Arbor, Michigan 48106*

(Received 19 May 1977)

Numerical hydrodynamic simulations which include absorption and transport modifications due to ion-acoustic turbulence have been performed. These simulations can reproduce the important features of the fast-ion velocity distributions as measured with biased charge collectors and a magnetic spectrograph in spherically illuminated microballoon experiments. Experiments with hemispherical targets show that a substantial amount of fast-ion energy is directed inward and may contribute to driving the implosion.

Measurements of ion expansion energy from laser-heated plasmas show an anomalous fast-ion component.<sup>1</sup> Charge collectors biased to record ion current as a function of time show that in a typical experiment approximately half of the absorbed energy resides in only a few percent of the target mass.<sup>2</sup> This result implies that the absorbed energy is being coupled into a very thin layer at the target surface. This mode of coupling leads to poor momentum transfer between the expanding plasma and the compressed region of the pellet and could place a fundamental limitation on the efficiency of laser-driven ablative compression.

Figure 1 presents data from two instruments used to obtain the ion velocity distribution. The target for this laser shot was a 54- $\mu\text{m}$ -diam spherical glass shell with 0.8- $\mu\text{m}$  wall thickness filled with 10 atm of DT gas mixture. The laser energy on the target was 21 J at 1.06- $\mu\text{m}$  wavelength in a 70-psec flat pulse. A lens-ellipsoidal-mirror illumination system provided near-normal illumination of the pellet.<sup>3</sup>

Figure 1(a) shows the voltage trace from a conventional charge collector. The initial sharp spike is produced by photoelectron emission from the collector surface due to the ultraviolet and x-ray flash when the laser pulse hits the target. The second peak results from the fast ions, and the broad feature represents the arrival of the bulk of the ionized target material. Using previously measured values for the mean ionic charge and secondary-emission coefficient,<sup>4</sup> this

voltage trace can be converted into an ion-velocity spectrum. Because of uncertainty in the secondary-emission correction, the velocity spectrum above  $2 \times 10^8$  cm/sec is obtained with a small magnetic spectrograph which uses cellulose nitrate foils as detectors.<sup>5</sup>

Figure 1(b) shows the ion-velocity spectrum. At high velocities, the spectrum is adequately

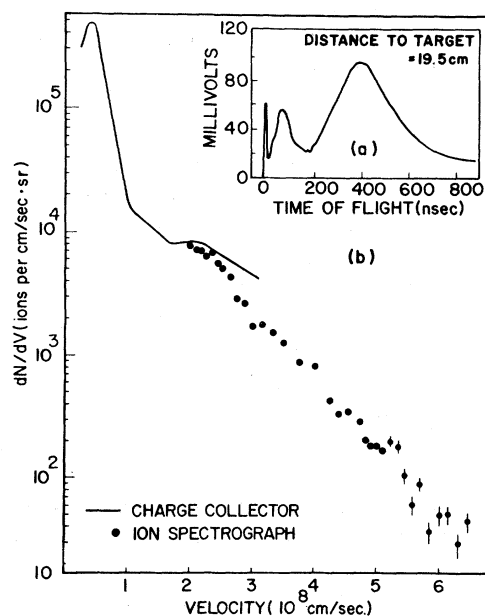


FIG. 1. (a) Oscilloscope voltage trace from a biased charge collector. (b) Composite ion-velocity spectrum from a charge collector and ion spectrograph.

represented by the exponential form  $dN/dv = A \times \exp(-v/v_0)$ , with scale velocity  $v_0 = 0.76 \times 10^8$  cm/sec. Similar spectra have been obtained from many target shots. Integrations of such spectra give about 6% of the target mass in the fast-ion group. Typically 15% of the incident laser energy is absorbed with half of the absorbed energy in fast ions. The concentration of this much energy in so little mass implies a severe restriction on the penetration of the energy into the pellet, a result consistent with recent measurements of thermal conduction in layered planar targets.<sup>6</sup>

In Ref. 2, a correlation was made between the exponential velocity spectrum of the fast ions and the spectrum derived from a simple similarity model of an isothermal rarefaction. Corona electron temperatures determined from this model range from 5 to 15 keV, similar to those inferred from hard-x-ray measurements.<sup>7</sup> Such high temperatures cannot be understood on the basis of inverse bremsstrahlung absorption and classical transport coefficients.

It is possible to estimate the reduction in conductivity necessary to produce the observed fast-ion energies. Assume that laser power  $P_L$  is being absorbed in a narrow region at the critical density. This energy is divided between expansion loss outward and thermal conduction inward. We can represent the expansion loss by the expression for an isothermal blowoff and, for simplicity, assume flux-limited thermal transport inward. Energy balance gives

$$P_L = f n_e \theta_e v_e + 4 n_e \theta_e C_s,$$

where the electron thermal speed is  $v_e = (2\theta_e/m_e)^{1/2}$ , the sound speed is  $C_s = (Z\theta_e/m_i)^{1/2}$ , and  $n_e$  is the electron number density ( $10^{21}$  cm<sup>-3</sup>). The observation that 50% of the absorbed energy goes into fast-ion expansion gives the flux limiter,  $f$ , in terms of the square root of the electron-ion mass ratio,

$$f = 4(Zm_e/2m_i)^{1/2} \approx 1/21.$$

This represents a substantial reduction in heat flow<sup>8</sup> from the classical value.

The reduced heat flow results in a high corona temperature which can be estimated from

$$P_L \approx 2 \times (4n_e \theta_e C_s) = 3 \times 10^{13} \theta_e^{3/2} \text{ W/cm}^2.$$

For an absorbed power of  $7.5 \times 10^{14}$  W/cm<sup>2</sup>, the corona temperature becomes 8.5 keV, a value consistent with the temperature range inferred from the ion-velocity spectra.

An enhanced collision frequency in the neighborhood of the critical density would both lower the conductivity and increase the absorption. It has been suggested that ion-acoustic turbulence is responsible for these effects.<sup>8-12</sup> A spherical hydrodynamic simulation model which includes ion turbulence has been developed and found to reproduce the principal features of the experimental data.

As hot electrons from the laser deposition region flow into the cool interior of the pellet, they can trigger the growth of ion-acoustic instability. The criterion for the growth of ion waves is well known and is based on the ratio of the electron drift speed  $v_D$  to the phase velocity of ion waves  $V = \omega/k$ .<sup>13</sup> When the heat flow increases to the point where the electron drift speed is comparable to the ion-acoustic speed, the turbulence grows and inhibits further increase of the electron drift. This leads naturally to a flux limiter based on the electron-ion mass ratio as suggested by the fast-ion measurements.

In the simulation code it is assumed that the wave spectrum is narrowly peaked about the linearly fastest-growing mode for which  $k^2 \lambda_D^2 = \frac{1}{2}$ , where  $k$  is the wave number and  $\lambda_D$  the Debye length. The heat flux  $Q$  is first computed classically, subject to a flux limiter with  $f = \frac{1}{2}$ , and the electron drift speed estimated from  $v_D = |Q| / (\frac{1}{2} n_e \theta_e)$ . The drift speed and the ion phase velocity are then used in the dispersion relation<sup>13</sup> to determine the regions of the plasma which are unstable to the growth of ion waves. Since the growth rate is rapid compared to the hydrodynamic time scale, it is assumed that the turbulence is either absent or stabilized at its saturation value in different regions. The amplitude of the ion waves is limited by the trapping condition<sup>12</sup>

$$\delta n/n = \frac{1}{2} [(1 + k^2 \lambda_D^2)^{-1/2} - (3\theta_i/Z\theta_e)^{1/2}]^2,$$

where  $\delta n$  is the density fluctuation associated with the waves. The simulations show that ion turbulence occurs in the region extending outward from just inside the critical-density surface with density fluctuations on the order of 0.1–0.2.

By assuming that ion turbulence results in charge bunching, a simple estimate of conductivity by enhanced collision frequency can be obtained. We find the following expression:

$$K = K_{cl} / (1 + 30 \lambda_D^3 n_i \Delta^2),$$

where  $K_{cl}$  is the classical conductivity and  $\Delta = \delta n/n$ . This result is close to that obtained by Manheimer.<sup>11</sup> The simulation results show conduc-

tivity values which range from about  $K_{cl}/300$  at the critical-density point down to  $K_{cl}/2000$  in the outer regions of the corona.

Dawson and Oberman<sup>14</sup> have calculated the increase in effective collision frequency over the classical value for light absorption by a spectrum of ion waves with the result

$$\frac{\nu_{eff}}{\nu_{cl}} = \frac{\Delta^2}{4\pi} \frac{k}{\Delta k} n_i k^{-3}.$$

We assume a modest width for the wave spectrum,  $k/\Delta k \approx 2$ , about the linearly fastest-growing mode and use the above expression together with inverse bremsstrahlung for collisional absorption in the simulation code. A similar approach has been described by Faehl and Kruer.<sup>12</sup> In these calculations we have intentionally omitted profile steepening by the ponderomotive force and resonance absorption in order to isolate the effects due to ion turbulence.

Simulation-code results are shown in Fig. 2 for the case of a 55- $\mu\text{m}$ -diam glass-shell target similar to those used in the experiments. Figure 2(a) shows the computed charge-collector trace

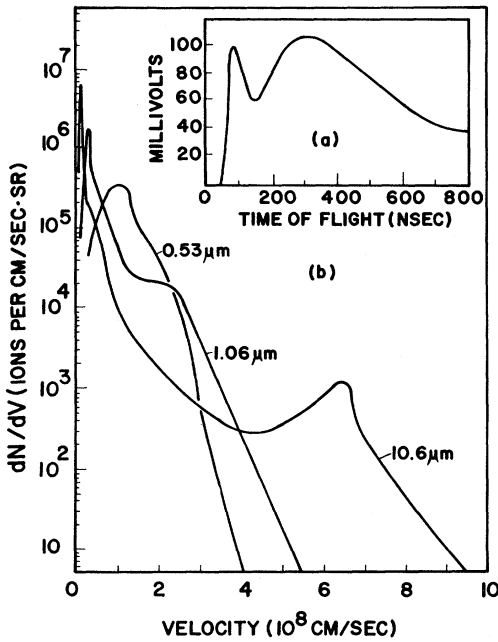


FIG. 2. (a) Simulation of the charge-collector response for the experiment illustrated in Fig. 1. (b) Simulation of the ion spectrum for the conditions used in (a) together with the same laser power at wavelengths of 0.53 and 10.6  $\mu\text{m}$ . The absorbed energies were 10.35 J at 0.53  $\mu\text{m}$ , 6.1 J at 1.06  $\mu\text{m}$ , and 2.2 J at 10.6  $\mu\text{m}$ ; the neutron yields were  $1.9 \times 10^8$ ,  $6.0 \times 10^7$ , and  $4.4 \times 10^2$ , respectively.

which, except for the ultraviolet flash, agrees quantitatively with the measured form of Fig. 1(a). In Fig. 2(b) are shown the computed velocity spectra for three laser wavelengths: 0.53, 1.06, and 10.6  $\mu\text{m}$ . The ion-turbulence model predicts a progressive hardening of the fast-ion spectrum as the laser wavelength is increased, which suggests that turbulence effects can be ameliorated by going to shorter wavelengths. Percentage absorptions given by the model for these three wavelengths are 24%, 15%, and 5.5%. Ion-turbulence calculations based on the model described in Ref. 11 resulted in much higher fractional absorption when applied to planar-target experiments.<sup>15</sup>

Fast ions from spherical-target experiments have recently been imaged in a pinhole camera using cellulose nitrate film detectors.<sup>16</sup> These images indicate a very broad angular distribution of fast-ion emission from each point on the emitting surface, leading to the speculation that some fast ions might be transported inward from the laser absorption region. Inwardly directed fast ions could affect the energy-deposition profile in the shell, since their range is well matched to the shell thickness.

To test this speculation we have performed eight experiments on glass hemispheres of 0.7- to 1.4- $\mu\text{m}$  wall thickness illuminated on the convex side with 1.06- $\mu\text{m}$  laser light and have observed fast ions from the unilluminated side in

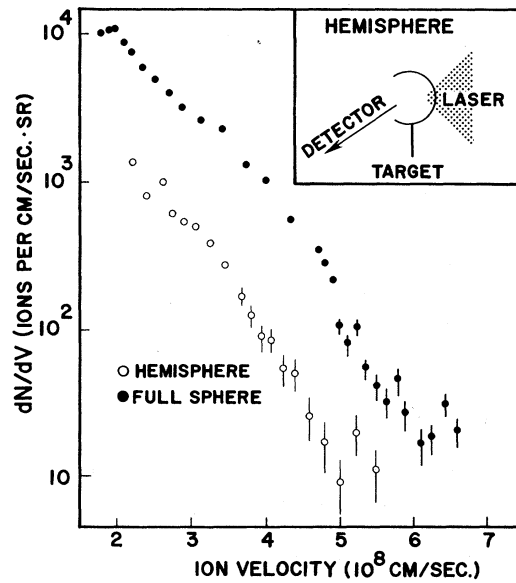


FIG. 3. Ion-velocity spectra from the inside surface of a hemisphere illuminated on one side compared to the spectrum from a similar-sized, fully illuminated sphere.

every case. Figure 3 shows the ion spectrum from one such shot, along with a companion spectrum from a fully illuminated spherical target of identical size. It is not possible in this experiment to determine whether the inwardly directed ions originated in the laser-deposition region and penetrated the shell or were drawn off the inside surface by fast electrons,<sup>17</sup> or by some other mechanism. If they do in fact originate in the absorption region, target designs could make use of this favorable energy-deposition profile to drive the implosion.<sup>18</sup>

This work was supported by the U. S. Energy Research and Development Administration under Contract No. ES-77-C-02-4149.

<sup>1</sup>A. Ehler, J. Appl. Phys. 46, 2464 (1975); J. S. Pearlman and J. P. Anthes, Bull. Am. Phys. Soc. 20, 1265 (1975); G. Charatis *et al.*, in *Proceedings of the Fifth International Conference on Plasma Physics and Controlled Nuclear Fusion Research, Tokyo, Japan, 1974* (International Atomic Energy Agency, Vienna, Austria, 1975), Vol. II, p. 317.

<sup>2</sup>P. Campbell, P. Hammerling, R. Johnson, J. Kubis, F. Mayer, and D. Slater, in *Proceedings of the Sixth International Conference on Plasma Physics and Controlled Nuclear Fusion Research, Berchtesgaden,*

West Germany, 1976 (to be published).

<sup>3</sup>C. Thomas, Appl. Opt. 14, 1267 (1975).

<sup>4</sup>R. Goforth, Rev. Sci. Instrum. 47, 451 (1976).

<sup>5</sup>D. Slater and F. Mayer, in *Fourth Workshop on Laser Interaction and Related Plasma Phenomena*, Troy, New York, 1976 (to be published).

<sup>6</sup>F. Young, R. Whitlock, R. Decoste, B. Ripin, D. Nagel, J. Stamper, J. McMahon, and S. Bodner, Appl. Phys. Lett. 30, 45 (1977); B. Yaakobi and T. C. Bristow, Phys. Rev. Lett. 38, 350 (1977); J. S. Pearlman, and J. P. Anthes, Appl. Phys. Lett. 27, 581 (1975).

<sup>7</sup>J. Kephart, R. Godwin, and G. McCall, Appl. Phys. Lett. 25, 108 (1974); F. C. Young, Phys. Rev. Lett. 33, 747 (1974); K. A. Brueckner, Phys. Rev. Lett. 36, 677 (1976).

<sup>8</sup>R. C. Malone, R. L. McCrory, and R. L. Morse, Phys. Rev. Lett. 34, 721 (1975).

<sup>9</sup>R. Bickerton, Nucl. Fusion 13, 457 (1973).

<sup>10</sup>R. L. Morse and R. C. Malone, Bull. Am. Phys. Soc. 21, 1028 (1976).

<sup>11</sup>W. M. Manheimer, Phys. Fluids 20, 265 (1977).

<sup>12</sup>R. Faehl and W. Kruer, Phys. Fluids 20, 55 (1977).

<sup>13</sup>N. Krall and A. Trivelpiece, *Principles of Plasma Physics* (McGraw-Hill, New York, 1973), p. 477.

<sup>14</sup>J. Dawson and C. Oberman, Phys. Fluids 6, 394 (1963).

<sup>15</sup>W. M. Manheimer, D. G. Colombant, and B. H. Ripin, Phys. Rev. Lett. 38, 1135 (1977).

<sup>16</sup>D. Slater, Appl. Phys. Lett. 31, 196 (1977).

<sup>17</sup>D. V. Giovanielli, Bull. Am. Phys. Soc. 21, 1047 (1976).

<sup>18</sup>R. Hofstadter, private communication.

## Generation of Whistler-Mode Radiation by Parametric Decay of Bernstein Waves

R. W. Boswell

*Space Science Department, European Space Agency, Noordwijk, The Netherlands*

and

M. Giles

*Space and Plasma Physics Group, University of Sussex, Sussex, England*

(Received 11 August 1976)

It is shown both experimentally and theoretically that a Bernstein wave can decay parametrically into another Bernstein wave and a whistler-mode wave. The process only occurs in a highly collisionless plasma and it is suggested that this is the dominant mechanism for producing whistler-mode noise in the auroral ionosphere.

In this Letter we present experimental and theoretical results showing that a Bernstein wave may parametrically decay into another Bernstein wave and a whistler-mode wave. This has not been previously considered and represents quite a departure from the generally held views on the nonlinear generation of electromagnetic waves.

That this interaction has not been observed be-

fore is probably due to the geometry of the transmitting antennas. Previous experiments<sup>1</sup> generally used gridded structures which launched waves with wave vectors essentially perpendicular to the grid. This experiment differs in that the antenna was a simple wire 7-cm-long aligned parallel to the ambient field  $\vec{B}_0$ , which allowed the Bernstein waves to propagate obliquely,